DOI: 10.1002/ange.201306881

Radical Ions

Isolation and Characterization of the Cycloparaphenylene Radical Cation and Dication**

*Eiichi Kayahara, Takahiko Kouyama, Tatsuhisa Kato, Hikaru Takaya, Nobuhiro Yasuda, and Shigeru Yamago**

Radical cations and dications of π-conjugated oligomers and polymers, such as poly(*para*-phenylene)s, poly(*para*-phenylenevinylene)s, and poly(thiophene)s, play a pivotal role as active constituents of charge-transporting layers in organic electronics, such as organic light-emitting diodes, organic semiconductors, organic solar cells, and single-molecule wires.[1] Their structure as well as the delocalization or localization of charge and spin in a molecule have been the subject of significant debate associated with the mechanism of charge transport. Significant progress has been made in isolating and characterizing π-radical cations and dications of oligomers with well-defined structures; these are used as models for polymers.[2] For example, the radical cations of poly(*para*-phenylene) oligomers were prepared and characterized by Rathore and co-workers.[3] They confirmed the delocalization of the positive charge over all phenylene moieties by size-dependent UV/Vis absorption spectroscopy and X-ray crystallographic analysis of the quaterphenyl derivative; from the alternation of the bond lengths and a decrease in the dihedral angle of the two nearly coplanar *para*-phenylene units, an increase in the quinoidal character could be deduced. However, the structure is asymmetric, and the positive charge is not evenly delocalized. Although they attributed this asymmetric character to the existence of a terminal structure, no definite experimental data were obtained to confirm this hypothesis. Nevertheless, radical cations of conjugated oligomers without terminal structures should be appropriate models for infinite polymers. However, no examples of such models have been reported to date.

Recently, significant progress has been made in the synthesis of cycloparaphenylenes (CPPs), which are end-free, cyclic versions of poly(*para*-phenylene)s.[4–7] These studies also determined various unique physical properties of CPPs, such as size-dependent photophysical properties[4b,6b,8] and size-complementary host–guest complex formation.[4f,9] The redox properties are among the most interesting characteristics of these compounds and suggest that the resulting radical cations and/or dications should be isolable in pure form.[10] However, several attempts to isolate them under electrochemical conditions have been unsuccessful. Herein, we report the isolation and characterization of the persistent radical cation [8]CPP$^{\bullet+}$ and the dication [8]CPP^{2+}, which were generated by chemical oxidation of [8]CPP for the first time (Scheme 1).

When [8]CPP ($E_{ox} = 0.59$ V vs. Fe/Fe$^+$) was treated with NOSbF$_6$ (1.0 equiv) in CH$_2$Cl$_2$ at room temperature, the reaction mixture immediately turned from pale greenish yellow into intense orange. After removal of the solvent, the resulting solid was collected by filtration and washed with

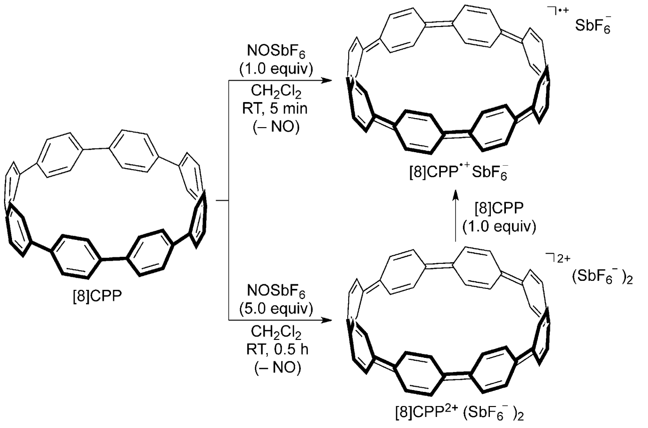

Scheme 1. Synthesis of the radical cation and dication of [8]CPP.

---

[*] Dr. E. Kayahara, Dr. H. Takaya, Prof. Dr. S. Yamago
Institute for Chemical Research, Kyoto University
Uji 611-0011 (Japan)
E-mail: yamago@scl.kyoto-u.ac.jp
Homepage: http://www.scl.kyoto-u.ac.jp/~kayahara/

Dr. E. Kayahara, Prof. Dr. S. Yamago
Core Research for Evolutional Science and Technology (CREST)
Japan Science and Technology Agency
Tokyo 102-0076 (Japan)

T. Kouyama, Prof. Dr. T. Kato
Graduate School of Human and Environmental Sciences
Kyoto University
Sakyo-ku, Kyoto 606-8501 (Japan)

Prof. Dr. T. Kato
Institute for Liberal Arts and Sciences, Kyoto University
Sakyo-ku, Kyoto 606-8501 (Japan)

Dr. N. Yasuda
Research and Utilization Division
Japan Synchrotron Radiation Research Institute
Hyogo 679-5198 (Japan)

[**] This work was partly supported by the CREST program of the Japan Science and Technology Agency (S.Y.) and by a Grant-in-Aid for Young Scientists (B) from the Japan Society for the Promotion of Science (E.K.). Single-crystal X-ray analysis was performed at BL40XU of SPring-8 with the approval of the Japan Synchrotron Radiation Research Institute (JASRI; 2013A1705). We thank Dr. Kunihisa Sugimoto (JASRI) and Dr. Katsuhiro Isozaki (Kyoto University) for their guidance for X-ray crystallographic analysis and Prof. Toshiyasu Suzuki (Institute for Molecular Science) for valuable discussions and suggestions.

Supporting information for this article is available on the WWW under http://dx.doi.org/10.1002/anie.201306881.

a CH_2Cl_2/hexane solution (1:1, *v*/*v*) to afford [8]CPP$^{\bullet+}$ SbF$_6^-$ as a brown solid in 76 % yield. The salt was sensitive to air, but stable under a nitrogen atmosphere at −30 °C for more than two weeks. The ^{1}H NMR spectrum of the salt was silent, which is consistent with the formation of a paramagnetic species.

First, the radical cation was characterized by UV/Vis/NIR spectroscopy in CH_2Cl_2 (Figure 1 a, —; NIR = near infrared); a large bathochromic shift relative to neutral [8]CPP[6b] and characteristic broad absorption bands in the NIR region (λ_{max} = 1770 nm) that extended up to approximately 2300 nm were observed. The shape of the absorption bands was insensitive to the concentration (0.1×10^{-4} M–1.2×10^{-4} M; Supporting Information, Figure S1), which suggests that the radical cation exists in a monomeric form.[2a,3a] Time-dependent (TD) DFT calculations indicated that the absorption in the NIR region at 1413 nm with an oscillator strength of f = 0.2608 is mainly due to a transition from the degenerate HOMOs to the SOMO (Figure 1 b, —).

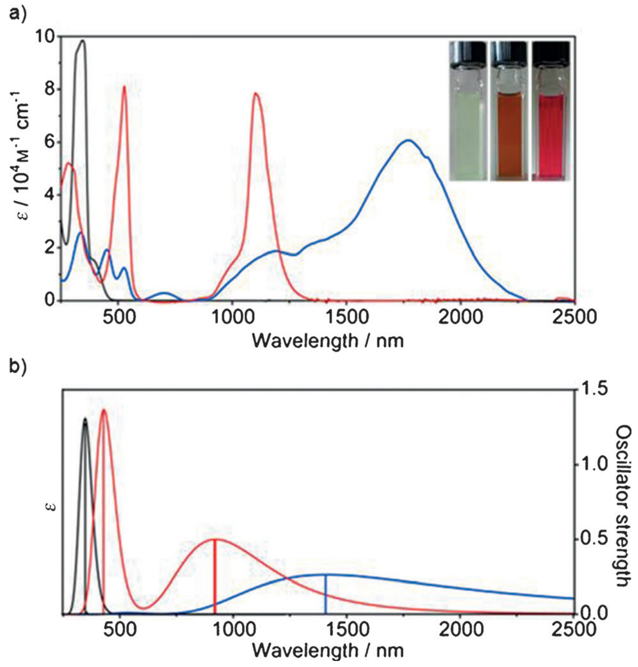

Figure 1. a) UV/Vis/NIR spectra of [8]CPP (—), [8]CPP$^{\bullet+}$ SbF$_6^-$ (—) and [8]CPP^{2+} (SbF$_6^-$)$_2$ (—) in CH_2Cl_2 (1.0×10^{-4} mol L^{-1}). Photographs of solutions of [8]CPP (left), [8]CPP$^{\bullet+}$ SbF$_6^-$ (center), and [8]CPP^{2+} (SbF$_6^-$)$_2$ (right) in CH_2Cl_2 (1.0×10^{-4} mol L^{-1}) under ambient light are also shown. b) UV/Vis/NIR spectra obtained by TD-DFT calculations at the (U)B3LYP/6-31G(d) level of theory.

The generation of the radical cation was unambiguously confirmed by electron spin resonance (ESR) spectroscopy. The ESR spectrum of [8]CPP$^{\bullet+}$ SbF$_6^-$ in CH_2Cl_2 solution (1.0×10^{-3} M) at 293 K showed a symmetrically split multiplet with a ^{1}H hyperfine coupling constant (hfcc) of 0.034 mT (Figure 2, —). These results suggest that the spin was fully delocalized over all of the CPP *para*-phenylene units. The simulated spectrum (—) was calculated by assuming that the 32 hydrogen atoms of [8]CPP are all equivalent and is perfectly superimposable on the observed spectrum. The *g* value was 2.0033, which is bigger than that of the free electron (2.0023). This difference implies that CPP$^{\bullet+}$ has a low-lying excited electronic state that is characterized by a hole-promoted configuration.

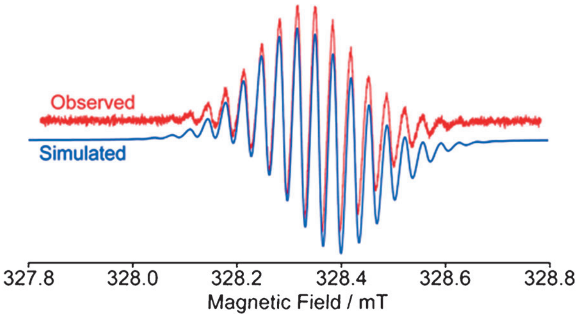

Figure 2. Observed (—) and simulated (—) ESR spectra of [8]CPP$^{\bullet+}$ SbF$_6^-$ in CH_2Cl_2 (1.0×10^{-3} M) at 293 K.

The dication of [8]CPP, [8]CPP^{2+} (SbF$_6^-$)$_2$, was isolated as a red-purple solid in 91 % yield by treatment of [8]CPP with an excess amount of NOSbF$_6$ (Scheme 1). The dication was also stable under a nitrogen atmosphere at −30 °C for more than one month, but gradually decomposed on exposure to air. As the dication is a closed-shell molecule, it was silent to ESR, but showed a characteristic singlet resonance at 5.24 ppm in the ^{1}H NMR spectrum recorded in CD_2Cl_2 at room temperature, which corresponds to a large upfield shift of the signal compared to that of neutral [8]CPP (7.52 ppm).[11] Furthermore, the shape of the resonance of the dication indicates that all phenylene units of the dication are equivalent within the time scale of the NMR measurement. Gauge-independent atomic orbital (GIAO) calculations also indicated an upfield shift of the resonances of [8]CPP^{2+} (3.3 and 7.0 ppm) relative to those of neutral [8]CPP (7.4 and 7.9 ppm).

The UV/Vis/NIR spectra of the dication in CH_2Cl_2 showed two distinct absorptions bands at λ_{max} = 1102 nm and λ_{max} = 528 nm; no absorption was observed in the NIR region (Figure 1 a, —).

TD-DFT calculations indicated that the longer-wavelength absorption at 923 nm with f = 0.4943 is due to the transition from the degenerate HOMOs to the LUMO, and that the shorter-wavelength absorption at 429 nm with f = 1.3496 corresponds to a transition from the HOMOs to the LUMO + 1 (Figure 1 b, —). The insensitivity of the absorption bands to the concentration suggests that the dication also exists in its monomeric form (Figure S2). The right choice of oxidant was crucial to obtain the radical cation in a pure form. For example, when [8]CPP was treated with SbCl$_5$ (1.5 equiv),[12] a mixture of [8]CPP$^{\bullet+}$ SbCl$_6^-$ and [8]CPP^{2+} (SbCl$_6^-$)$_2$ was formed. Although the resulting mixture was ESR-active and gave a spectrum identical to the one shown in Figure 2, the dication was the major component (ca. 95 %), as determined by UV/Vis/NIR spectroscopy.

The radical cation was also cleanly generated by the reaction of one equivalent of neutral [8]CPP with either [8]CPP^{2+} (SbF$_6^-$)$_2$ or [8]CPP^{2+} (SbCl$_6^-$)$_2$. The selective transformation was confirmed by UV/Vis/NIR spectroscopy by observing the disappearance of the characteristic twin peaks of the dication at 1102 and 528 nm and the appearance of the NIR absorption of the radical cation (see the Supporting Information). Two isosbestic points at 756 and 1258 nm were observed in titration experiments by the incremental addition of [8]CPP to a solution of [8]CPP^{2+}(SbF$_6^-$)$_2$ (Figure S5). This result is also consistent with quantitative conversion of the dication into the radical cation. Furthermore, the resulting sample solution clearly showed the ESR signals that are characteristic of the radical cation.

The structures and electronic configurations of [8]CPP$^{•+}$ and [8]CPP^{2+} were estimated by DFT calculations at the (U)B3LYP/6-31G(d) level of theory. Although five and three local minima were located for [8]CPP$^{•+}$ and [8]CPP^{2+}, respectively, only the most stable isomers are discussed here because all isomers are structurally related rotational isomers with respect to the phenylene units. The same arguments can be applied to the other isomers (see the Supporting Information).

The most stable isomers of [8]CPP$^{•+}$ and [8]CPP^{2+} possess a point group symmetry close to D_{4h}. The structures of the radical cation and the dication preserved the concentric circular shape of neutral CPP (see the Supporting Information); these results are consistent with full delocalization of spin and positive charge over all phenylene units. The dihedral angles of the adjacent two *para*-phenylene units of [8]CPP$^{•+}$ and [8]CPP^{2+} were 23° and 14°, respectively, and thus significantly smaller than that of neutral [8]CPP (30°; Table 1). Small contraction (1.0–2.0 %) of the C$_{ipso}$–C$_{ipso}$ and C$_{ortho}$–C$_{ortho}$ bonds and elongation of the C$_{ipso}$–C$_{ortho}$ bonds relative to those of the neutral compound were observed in both cases. These changes suggest an increase in the quinoidal contribution. The transition to the quinoidal form is more significant for the dication, probably owing to the necessity to delocalize two cationic charges over all phenylene units.

Table 1: Calculated C–C bond lengths, dihedral angles, and Mulliken spin densities and charges on the *ipso* and *ortho* carbon atoms of [8]CPP, [8]CPP$^{•+}$, and [8]CPP^{2+}.[a]

Parameter	[8]CPP[b]	[8]CPP$^{•+}$	[8]CPP^{2+}
Bond length[c] [Å]:			
C$_{ipso}$–C$_{ipso}$	1.4866	1.4716	1.4557
C$_{ipso}$–C$_{ortho}$	1.4075	1.4145	1.4229
C$_{ortho}$–C$_{ortho}$	1.3914	1.3847	1.3779
Dihedral angle[c] [°]:			
C$_{ortho}$–C$_{ipso}$–C$_{ipso}$–C$_{ortho}$	30.80	22.70	14.00
Mulliken spin density[c] (and charge[c]):			
C$_{ipso}$	– (–)	0.0454 (0.102)	– (0.107)
C$_{ortho}$	– (–)	0.0109 (−0.185)	– (−0.175)
	– (–)	0.0072 (−0.163)	– (−0.157)

[a] Calculated at the (U)B3LYP/6-31G* level of theory. [b] Data taken from Ref. [6b]. [c] Average values.

The equal distribution of spin and charges was further supported by an analysis of the Mulliken charge and spin densities. In the radical cation, the spin density is more localized on the *ipso* carbon atom, whilst the charge is more equally distributed between the *ipso* and *ortho* carbon atoms. Whereas spin density and charge of the *ortho* carbon atoms were slightly different, they can be time-averaged during ESR or NMR measurements (Table 2).

Table 2: C–C bond lengths and dihedral angles of [8]CPP^{2+} (SbCl$_6^-$)$_2$ and [8]CPP in the solid state.

Parameter	[8]CPP^{2+} (SbCl$_6^-$)$_2$	[8]CPP[a]
Bond lengths[b] [Å]:		
C$_{ipso}$–C$_{ipso}$	1.450(9)	1.485(8)
C$_{ipso}$–C$_{ortho}$	1.405(9)	1.401(4)
C$_{ortho}$–C$_{ortho}$	1.369(9)	1.382(8)
Dihedral angle[b] [°]:		
C$_{ortho}$–C$_{ipso}$–C$_{ipso}$–C$_{ortho}$	3.6(4)–6.6(5)	1.5(3), 24.0(3), 30.3(3), 41.4(7)

[a] Data taken from Ref. [4f]. [b] Average values.

The structure of [8]CPP^{2+} was determined by single-crystal X-ray crystallographic analysis, which was performed on a crystal obtained by vapor diffusion of toluene into a solution of [8]CPP^{2+}(SbCl$_6^-$)$_2$ in CH$_2$Cl$_2$ over three days. The crystal belongs to the tetragonal crystal system with a space group of $C2/m$ (Figure 3). The most striking structural feature of [8]CPP^{2+} is the coplanar arrangement of all *para*-phenylene units to form a belt-like structure. The dihedral angles of the neighboring *para*-phenylene units are in the range of 3.6(4)–6.6(5)° and significantly smaller than those observed for the neutral species (ca. 30.1° by calculation[6b] and 1.5(3)°, 24.0(3)°, 30.3(3)°, and 41.4(7)° by single-crystal X-ray analysis[4f]). Furthermore, the C$_{ipso}$–C$_{ipso}$ and C$_{ortho}$–C$_{ortho}$ bond lengths (1.450(9) and 1.369(9) Å) were shortened by 2.3 % and 0.9 %, respectively, relative to neutral [8]CPP. The C$_{ipso}$–C$_{ortho}$ bond length (1.405(9) Å) was slightly elongated by 0.3 %, compared with the neutral species (Table 2). These results are also consistent with the occur-

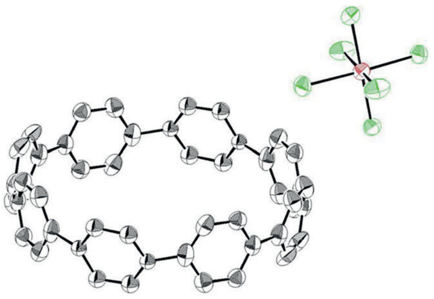

Figure 3. ORTEP drawing of [8]CPP^{2+} (SbCl$_6^-$)$_2$. Thermal ellipsoids set at the 50 % probability level. One fourth of the entire structure constitutes an asymmetric unit. Hydrogen atoms, solvent atoms, and some disordered toluene molecules were omitted for clarity. Some benzene rings and chlorine atoms on CPP and SbCl$_6$ are disordered over two equivalent positions, but only one of them is shown. Antimony red, carbon black, chlorine green.

rence of bond alternation. The [8]CPP^{2+} unit in the crystal structure is highly symmetric and preserves a circular shape. This structure also supports complete delocalization of the cationic charge over all *para*-phenylene units. The counter anion $SbCl_6^-$ was located at the exterior of [8]CPP^{2+}, whose cavity was occupied by toluene molecules.

The X-ray structure was different from that of the most stable conformer of [8]CPP^{2+} obtained by the calculations. Furthermore, the dihedral angles of two adjacent *para*-phenylene units were slightly different, although the bond lengths were in good agreement with those of the calculated structure. The differences are most likely due to the absence of the counter ion in the calculation, but effects of crystal packing may also contribute to some extent. In any case, characteristic structural features are essentially the same in the X-ray structure and its calculated variant.

The molecular arrangement of [8]CPP^{2+} $(SbCl_6^-)_2$ in the crystal is shown in Figure 4. The CPP rings are tiled on an *ab* plane with close packing and stacked with the central axes of the CPP rings aligned along the *c* axis to form a honeycomb-shaped tubular structure (Figure 4a,b). The counter anion $SbCl_6^-$ occupies a void space that consists of two layers of CPP sheets to form another layer of an anionic $SbCl_6^-$ sheet. The nearest-neighbor intermolecular distance between CPPs is 3.38(2) Å (Figure 4c), which is slightly smaller than the sum of the van der Waals radii of sp^2-hybridized carbon atoms.

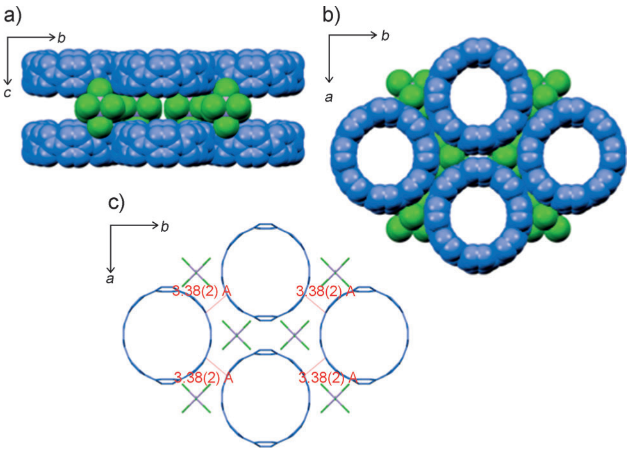

Figure 4. a,b) Crystal packing of [8]CPP^{2+} $(SbCl_6^-)_2$. View along the a) *a* axis and the b) *c* axis. c) Intermolecular aromatic–aromatic interactions in the crystal of [8]CPP^{2+} $(SbCl_6^-)_2$. Antimony red, carbon blue, chlorine green. For clarity, hydrogen atoms and solvent molecules were omitted.

In summary, the radical cation and dication of [8]CPP were successfully synthesized by one- or two-electron chemical oxidation of [8]CPP with $NOSbF_6$ or $SbCl_5$. They are surprisingly stable, and in-depth analysis revealed that the cationic charge and the spin are fully delocalized over all *para*-phenylene units. Although many radical cations and dications of π-conjugated oligomers have been isolated, this is the first time that a monomeric radical cation and dication have been isolated without steric protection. Further studies to elucidate the nature of the oxidized species, including their chemical reactivities, are underway.

Received: August 6, 2013
Revised: September 18, 2013

Keywords: nanobelts · oxidation · quinodimethanes · radical ions · X-ray diffraction

---

[1] a) J. L. Brédas, G. B. Street, *Acc. Chem. Res.* **1985**, *18*, 309–315; b) L. M. Tolbert, *Acc. Chem. Res.* **1992**, *25*, 561–568; c) R. E. Martin, F. Diederich, *Angew. Chem.* **1999**, *111*, 1440–1469; *Angew. Chem. Int. Ed.* **1999**, *38*, 1350–1377; d) A. C. Grimsdale, K. L. Chan, R. E. Martin, P. G. Jokisz, A. B. Holmes, *Chem. Rev.* **2009**, *109*, 897–1091; e) J. Heinze, B. A. Frontana-Uribe, S. Ludwigs, *Chem. Rev.* **2010**, *110*, 4724–4771.

[2] a) T. Nishinaga, K. Komatsu, *Org. Biomol. Chem.* **2005**, *3*, 561–569; b) T. Nishinaga, A. Wakamiya, D. Yamazaki, K. Komatsu, *J. Am. Chem. Soc.* **2004**, *126*, 3163–3174; c) D. Yamazaki, T. Nishinaga, N. Tanino, K. Komatsu, *J. Am. Chem. Soc.* **2006**, *128*, 14470–14471; d) F. Marchetti, C. Pinzino, S. Zacchini, G. Pampaloni, *Angew. Chem.* **2010**, *122*, 5396–5400; *Angew. Chem. Int. Ed.* **2010**, *49*, 5268–5272; e) X. Chen, B. Ma, X. Wang, S. Yao, N. L. Z. Zhou, Y. Li, W. Huang, J. Ma, J. Zuo, X. Wang, *Chem. Eur. J.* **2012**, *18*, 11828–11836; f) X. Chen, B. Ma, S. Chen, Y. Li, W. Huang, J. Ma, X. Wang, *Chem. Asian J.* **2013**, *8*, 238–243.

[3] a) M. Banerjee, S. V. Lindeman, R. Rathore, *J. Am. Chem. Soc.* **2007**, *129*, 8070–8071; b) M. Banerjee, R. Shukla, R. Rathore, *J. Am. Chem. Soc.* **2009**, *131*, 1780–1786.

[4] a) E. S. Hirst, R. Jasti, *J. Org. Chem.* **2012**, *77*, 10473–10478; b) R. Jasti, J. Bhattacharjee, J. B. Neaton, C. R. Bertozzi, *J. Am. Chem. Soc.* **2008**, *130*, 17646–17647; c) T. J. Sisto, M. R. Golder, E. S. Hirst, R. Jasti, *J. Am. Chem. Soc.* **2011**, *133*, 15800–15802; d) E. R. Darzi, T. J. Sisto, R. Jasti, *J. Org. Chem.* **2012**, *77*, 6624–6628; e) J. Xia, R. Jasti, *Angew. Chem.* **2012**, *124*, 2524–2526; *Angew. Chem. Int. Ed.* **2012**, *51*, 2474–2476; f) J. Xia, J. W. Bacon, R. Jasti, *Chem. Sci.* **2012**, *3*, 3018–3021.

[5] a) H. Omachi, Y. Segawa, K. Itami, *Acc. Chem. Res.* **2012**, *45*, 1378–1389; b) H. Takaba, H. Omachi, Y. Yamamoto, J. Bouffard, K. Itami, *Angew. Chem.* **2009**, *121*, 6228–6232; *Angew. Chem. Int. Ed.* **2009**, *48*, 6112–6116; c) H. Omachi, S. Matsuura, Y. Segawa, K. Itami, *Angew. Chem.* **2010**, *122*, 10400–10403; *Angew. Chem. Int. Ed.* **2010**, *49*, 10202–10205; d) Y. Segawa, S. Miyamoto, H. Omachi, S. Matsuura, P. Šenel, T. Sasamori, N. Tokitoh, K. Itami, *Angew. Chem.* **2011**, *123*, 3302–3306; *Angew. Chem. Int. Ed.* **2011**, *50*, 3244–3248; e) Y. Segawa, P. Šenel, S. Matsuura, H. Omachi, K. Itami, *Chem. Lett.* **2011**, *40*, 423–425; f) Y. Ishii, Y. Nakanishi, H. Omachi, S. Matsuura, K. Matsui, H. Shinohara, Y. Segawa, K. Itami, *Chem. Sci.* **2012**, *3*, 2340–2345.

[6] a) S. Yamago, Y. Watanabe, T. Iwamoto, *Angew. Chem.* **2010**, *122*, 769–771; *Angew. Chem. Int. Ed.* **2010**, *49*, 757–759; b) T. Iwamoto, Y. Watanabe, Y. Sakamoto, T. Suzuki, S. Yamago, *J. Am. Chem. Soc.* **2011**, *133*, 8354–8361; c) E. Kayahara, Y. Sakamoto, T. Suzuki, S. Yamago, *Org. Lett.* **2012**, *14*, 3284–3287; d) E. Kayahara, T. Iwamoto, T. Suzuki, S. Yamago, *Chem. Lett.* **2013**, *42*, 621–623.

[7] a) B. D. Steinberg, L. T. Scott, *Angew. Chem.* **2009**, *121*, 5504–5507; *Angew. Chem. Int. Ed.* **2009**, *48*, 5400–5402; b) M. Iyoda, J. Yamakawa, M. J. Rahman, *Angew. Chem.* **2011**, *123*, 10708–10740; *Angew. Chem. Int. Ed.* **2011**, *50*, 10522–10553; c) U. H. F. Bunz, S. Menning, N. Martín, *Angew. Chem.* **2012**, *124*, 7202–7209; *Angew. Chem. Int. Ed.* **2012**, *51*, 7094–7101.

[8] a) M. Fujitsuka, D. W. Cho, T. Iwamoto, S. Yamago, T. Majima, *Phys. Chem. Chem. Phys.* **2012**, *14*, 14585 – 14588; b) Y. Segawa, A. Fukazawa, S. Matsuura, H. Omachi, S. Yamaguchi, S. Irle, K. Itami, *Org. Biomol. Chem.* **2012**, *10*, 5979 – 5984; c) T. Nishihara, Y. Segawa, K. Itami, Y. Kanemitsu, *J. Phys. Chem. Lett.* **2012**, *3*, 3125 – 3128; d) M. Fujitsuka, T. Iwamoto, E. Kayahara, S. Yamago, T. Majima, *ChemPhysChem* **2013**, *14*, 1570 – 1572.

[9] T. Iwamoto, Y. Watanabe, T. Sadahiro, T. Haino, S. Yamago, *Angew. Chem.* **2011**, *123*, 8492 – 8494; *Angew. Chem. Int. Ed.* **2011**, *50*, 8342 – 8344.

[10] Preliminary investigations suggest that the single peak observed in CV measurements as shown in Ref. [6b,c] is most likely due to a two-electron process rather than a one-electron process. Details will be reported in due course.

[11] Signals of the carbon atoms could not be detected by ^{13}C NMR spectroscopy owing to the low solubility of the dication.

[12] R. Rathore, S. V. Lindeman, A. S. Kumar, J. K. Kochi, *J. Am. Chem. Soc.* **1998**, *120*, 6931 – 6939.